Research Article

Humaira Rizwana*, Najat A. Bokahri, Ahmed Alfarhan, Horiah A. Aldehaish, and Noura S. Alsaggabi

Biosynthesis and characterization of silver nanoparticles prepared using seeds of *Sisymbrium irio* and evaluation of their antifungal and cytotoxic activities

https://doi.org/10.1515/gps-2022-0048
received January 31, 2022; accepted April 06, 2022

Abstract: Recent studies have shown that green synthesis of silver nanoparticles (AgNPs) and their application in the control of phytopathogenic fungi is a burgeoning field. *Sisymbrium irio* (Si) (London rocket) is a well-known weed that grows abundantly in Saudi Arabia from February to May. The present study is concerned with the rapid synthesis of silver nanoparticles from the aqueous seed extract of Si) in the presence of sunlight. The biosynthesized Si-AgNPs were characterized using UV-Visible spectroscopy (UV-Vis), energy dispersive X-ray (EDX) microanalysis, dynamic light scattering analysis (DLS), transmission electron microscopy (TEM), and Fourier transform infrared spectroscopy analysis (FTIR). The UV-Vis spectrum revealed a prominent surface plasmon resonance (SPR) absorption band (~439 nm) characteristic of AgNPs. As revealed by TEM analysis, the Si-AgNPs were predominantly spheroidal in shape and measured between 4 and 51 nm, while the *Z* average of nanoparticles was 94.81 nm as revealed by the DLS spectrum. The FTIR spectrum displayed peaks related to important functional groups (amines, phenols, carboxylic acids, flavonoids, aromatic compounds, and esters) that aid in the reduction, encapsulation, and stability of AgNPs. The Si-AgNPs were further investigated against a panel of potent fungal phytopathogens that included *Alternaria alternata*, *A. brassicae*, *Fusarium solani*, *F. oxysporum*, and *Trichoderma harzianum*. The cytotoxic activity of the biosynthesized nanoparticles against human cervical cancer cell lines (HeLa) was also tested. Si-AgNPs at 80 $\mu g \cdot mL^{-1}$ demonstrated a marked reduction in mycelial growth and spore germination. Similarly, Si-AgNPs exhibited dose-dependent cytotoxic activity against the HeLa cell line, with an IC_{50} value of 21.83 ± 0.76 $\mu g \cdot mL^{-1}$. The results of the present study demonstrate the robust cytotoxic and antifungal activities of Si-AgNPs. Based on the findings, Si-AgNPs can be exploited to design formulations that can effectively act as anticancer agents, controlling the proliferation of cancer cells while also combating fungal phytopathogens. However, future research to understand their toxicity mechanisms is needed.

Keywords: *Sisymbrium irio*, aqueous seed extract, silver nanoparticles, antifungal activity, cytotoxicity

1 Introduction

Nanotechnology involves the engineering of nano-sized particles (1–100 nm) using several chemical, physical, and biological methods [1]. Metals are used in the creation of nanoparticles because of their exceptional physiochemical properties like size, shape, conductivity, and most importantly, the surface volume ratio [2]. During the last decade, nanoparticles (NPs) synthesized using different metals have been used in various sports equipment, cosmetics, sunscreens, and textiles [3]. Recently, the application of nanotechnology has also been widened to drug delivery, management of diseases in humans and plants, in the food sector, and water safety [4]. However, a major concern with nanoparticles synthesized using conventional methods is the biological risks associated with toxicity and negative environmental effects [5]. As a result, plant extracts are being studied extensively around the world for their potential applications in medicine, nutraceuticals, and agriculture.

* **Corresponding author: Humaira Rizwana,** Department of Botany and Microbiology, College of Science, King Saud University, P.O. Box 22452, Riyadh 11495, Saudi Arabia, e-mail: hrizwana@ksu.edu.sa
Najat A. Bokahri, Ahmed Alfarhan, Horiah A. Aldehaish, Noura S. Alsaggabi: Department of Botany and Microbiology, College of Science, King Saud University, P.O. Box 22452, Riyadh 11495, Saudi Arabia

Fungal plant pathogens are one of the worst enemies of plants, as they cause several infections and diseases, incurring huge economic losses to plants and their produce. Major losses of fruits and vegetables occur during various stages of the postharvest period, which directly affect the quantity and quality, thus impacting their market value [6]. Additionally, some fungal pathogens produce mycotoxins, which are a great threat to human and animal health due to their adverse negative effects [7]. According to a recent Food and Agriculture Organization study, nearly 14% of food is lost due to postharvest diseases. Nevertheless, this excludes the retail stage [8]. In the agricultural sector, the most common method of controlling fungal postharvest losses is by the application of synthetic fungicides. However, the misuse of these chemical substances due to the recent demand for food supply globally has raised concerns as these chemical substances pose serious potential risks to all living organisms, water bodies, and the environment [9]. Hence, safer alternatives derived from natural compounds will serve as a boon in the given circumstances.

Plants possess a wide variety of bioactive secondary metabolites. Consequently, plant extracts are exploited to create NPs via a reduction process using various metals and metal oxides such as zinc, silver, gold, iron, copper, and platinum [10,11]. Previous studies have documented the green synthesis of nanoparticles using different parts of plants, such as fruits [12], seeds [13], flowers [14], leaves [15], and roots [16]. Amongst all the metals, silver is the most widely researched and used due to its low toxicity, antibacterial, antifungal, anti-inflammatory, and catalytic properties [17]. Plant-mediated synthesized nanoparticles have yielded promising results as antibacterial, anticancer, and antifungal agents [18,19]. Phyto-fabricated nanoparticles are gaining popularity as an excellent eco-friendly alternative to the conventional method of synthesis and biological methods because they are quick to create, cost-effective, safe, and use widely available plant material.

Sisymbrium irio L. is a member of the Cruciferae family and is also known as the London rocket. In Saudi Arabia, the plant is widely distributed [20], and is often abundant in open areas, along roadsides, and in neglected places. This weed grows abundantly from February to May. It bears dark green lobed leaves, clustered yellow flowers at the stem top, and long pods which bear very minute (0.6–1.2 mm) seeds. *S. irio* is a well-known plant in Unani and alternative folk medicine. Its leaves, stems, and seeds are used to treat various ailments, including rheumatism, inflammation, chest congestion, and cough, as an antiseptic, and as liver detoxicants [21,22]. Leaves and seeds are used to treat fever; they serve as an analgesic and possess antimicrobial properties [21,23]. In Unani medicine and Ayurveda, the seeds are used to treat hoarseness of voice, asthma, as a decongestant, and as an aphrodisiac. In this study, *Sisymbrium irio* L. seeds were used as plant material for the synthesis of silver NPs, and the resulting *Sisymbrium irio* NPs (Si-AgNPs) were characterized using UV-Vis spectroscopy (UV-Vis), energy dispersive X-ray (EDX) microanalysis, dynamic light scattering analysis (DLS), transmission electron microscopy (TEM), and Fourier transform infrared spectroscopy analysis (FTIR). The synthesized Si-AgNPs were investigated for their antifungal properties against a panel of potent fungal phytopathogens by the poison food technique and evaluated for their cytotoxic properties by the MTT assay. To our knowledge, no study has demonstrated the antifungal properties of Si-AgNPs against phytopathogens.

2 Materials and methods

2.1 Plant material

Si plants were collected from the campus of King Saud University, Kingdom of Saudi Arabia. The plant was deposited in the herbarium of the Department of Botany, College of Science, King Saud University, Saudi Arabia, under the voucher number 23318. The seeds were removed from the dried pods and used in this study.

2.2 Chemicals

The chemical compounds, media, and reagents used in the present study were pure and of analytical grade. Potato dextrose agar was procured from Sigma-Aldrich (St. Louis, MO, USA). Silver nitrate (≥99.5% purity) was purchased from Hi-Media Laboratories Pvt. Ltd (Mumbai, India). For all the experiments, analytical grade reagents and ultrapure water (Milli-Q) were used.

2.3 Preparation of aqueous seed extract

Dried seeds of Si were grounded coarsely in an electric grinder. Seed extract was prepared by adding 10 g of seed powder to 100 mL of distilled water. The mixture was heated at 60°C for 10 min. After the mixture cooled, it

was centrifuged at 5,000 rpm for about 5 min, filtered through Whatman's paper filter (No. 1) and used for the synthesis of AgNPs [24].

2.4 Biosynthesis of Si-AgNPs

The Si-AgNPs were synthesized by combining 10 mL of freshly prepared Si aqueous seed extract with 90 mL of silver nitrate ($AgNO_3$) solution (1 mM). The $AgNO_3$ solution was prepared by adding 0.008 g $AgNO_3$ to 50 mL of distilled water, and then 5 mL of Si seed extract was added at room temperature of 28°C with constant stirring. The mixture was immediately kept in sunlight. The color transition process was closely monitored and the time taken to change the original pale yellow to brown was noted. The formation of Si-AgNPs was confirmed using UV-Vis spectroscopic analysis after the mixture's color stabilized to a dark shade of brown [5].

2.5 Characterization of synthesized Si-AgNPs

Characterization of the synthesized Si-AgNPs was carried out with UV-Vis, TEM, DLS, EDX, FTIR, and field emission scanning electron microscope (FE-SEM). The formation of synthesized AgNPs was assessed visually for color changes and ascertained with a UV-Vis spectrophotometer (model: Thermo Scientific, 1500, USA). The sample mixture was analyzed for its absorbance at a wavelength range of 200–800 nm. The actual size and morphology of Si-AgNPs were observed under the TEM(JEOL). Sample preparation for TEM was carried out by adding synthesized Si-AgNPs to a copper grid and screening under the TEM (JEOL-JEM-1400 Plus, Tokyo, Japan). All the abovementioned preparations were carried out according to the instructions given by the manufacturer.

A DLS analyzer (Malvern Panalytical Zetasizer model Nano-ZS-90, Malvern, UK) was used to determine the distribution of synthesized Si-AgNPs and to measure their size. The DLS techniques were conducted by following the manufacturer's instructions. Synthesized particles were further characterized for their elemental composition with a FE-SEM (model no-JSM-7610F, Japan) equipped with an EDX detector. In brief, a thin film of Si-AgNPs was prepared on a glass slide, coated with platinum, and observed and photographed at an accelerating voltage (30 kV). FTIR spectroscopy analysis of Si seed extract and synthesized Si-AgNPs was carried out on a Thermo Scientific-Nicolet-6700, USA, spectrophotometer (400–4,000 cm^{-1}) with a KBr pellet [15].

2.6 Fungal pathogens

The fungal pathogens used in this study were provided by Department of Plant Protection, College of Food and Agricultural Sciences, King Saud University, Riyadh, Saudi Arabia. The following pathogens were screened in the present study: *Alternaria alternata*, *A. brassicae*, *Fusarium solani*, *Fusarium oxysporum*, and *Trichoderma harzianum*.

2.7 Mycelial growth inhibition

The antifungal activity of the synthesized Si-AgNPs was evaluated against selected fungal phytopathogens. The inhibitory activity of Si-AgNPs against test isolates was determined following the method described by Nguyen et al. [25], with some minor modifications. In brief, the AgNP suspension was prepared by adding Si-AgNPs to double sterilized distilled water, as previously described [26]. Various concentrations of Si-AgNPs (10, 20, 40, and 80 $\mu g \cdot mL^{-1}$) were prepared and screened for their inhibitory effect on the mycelial growth. Briefly, the Si-AgNPs suspension was mixed with sterilized potato dextrose agar (PDA), and the resulting mixture was added carefully to sterile Petri dishes and then allowed to cool and solidify.

After solidification, a 6 mm agar disc of the test pathogen was placed in the center of the plate. The agar plug was removed from a 7 days old fungal culture plate of the test pathogen. Plates containing PDA were inoculated with the agar plug of the test pathogen and treated with the fungicide (carbendazim-2%) which acted as a positive control, while sterilized distilled water was used as negative control. All the inoculated plates were incubated at 28°C (7 days). On the 7th day, the mycelial growth was measured and the percentage mycelial growth was calculated as follow:

$$\text{Percentage mycelial inhibition} = (Dpfc - Dpft)/Dpfc \times 100 \quad (1)$$

where *Dpfc*: average increase in mycelial growth in control, *Dpft*: average increase at each treatment.

2.8 Effect of Si-AgNPs on spore germination of test pathogens

Various concentrations of synthesized Si-AgNPs (10, 20, 40, and 80 μg·mL^{-1}) were tested to assess their effect on the spore germination of the test pathogens [27]. Spore suspension was prepared by following the method of Rizwana [28]. Concisely, spore suspension (500 μL) with a spore density of 1×10^6 spores·mL^{-1} was added to the same volume of Si-AgNPs in a sterile test tube with a final test concentration of 10, 20, 40, and 80 μg·mL^{-1} [28,29]. Spore suspension with sterile distilled water and carbendazim (2%) served as negative and positive controls. All the test tubes were placed in an incubator (28°C for 24 h) in the dark. After 24 h, the germination rate was recorded. On a clean slide, a drop of the fungal stain (lactophenol cotton blue) was added to observe spore germination under the light microscope. Percent inhibition of spore germination was calculated by counting 100 spores for each control and treatment [28,29]. The experiment was repeated thrice with all the fungal test isolates separately, with three replicates in each set.

2.9 Cytotoxic effect of Si-AgNPs against cervical cancer cell line.

The MTT (3-[4,5-dimethylthiazole-2-yl]-2,5-diphenyltetrazolium bromide) assay was used to assess the cytotoxicity of Si-AgNPs against HeLa cancer cells (human cervical cancer cell line) [30]. The HeLa cells were procured from the American Type Culture Collection (ATCC, USA). Precisely, HeLa cell lines at a density of 1×10^4 cells/well in 90 μL of Dulbecco's Modified Eagle Medium (DMEM) were added to a 96-well plate and allowed to settle for 24 h. Subsequently, the HeLa cells in the wells of the plate were treated with various concentrations (two-fold dilution) of Si-AgNPs ranging between 3.125 and 100 μg·mL^{-1} and incubated for 24 h. After the incubation, MTT was added to the wells and the plate was further incubated for another 4 h. Finally, 200 μL of DMSO was added to the reaction mixture in each well and thoroughly mixed. Optical density values were taken at 550 nm and percentage cell viability was determined with the help of a microplate reader (SunRise, TECAN, Inc, San Bruno, CA, USA). Each experiment was run thrice, and the control (negative) showed 100% cell viability. The inhibitory concentration (IC_{50}) was assessed using XLSTAT version 2021.5, and a graph showing the dose-dependent response was generated using regression analysis [31].

2.10 Statistical analysis

All the findings in this study were analyzed by the programme XLSTAT (software version 2020.1.1). The antimicrobial and cytotoxic activity data presented in this study are averages of three replicates and are expressed as standard deviation (±SD). All the values shown in figures (graphs) and tables (including colony diameter, % inhibition of mycelial growth, and spore germination) were determined by analysis of variance (ANOVA) for significant differences ($P \leq 0.05$) and Tukey's HSD test.

3 Results and discussion

3.1 Formation of Si-AgNPs and UV-Vis analysis

In the current study, the formation of Si-AgNPs was accomplished by adding the aqueous seed extracts of Si to an $AgNO_3$ solution. The color transition process was closely monitored. Within 7 min of exposure to direct sunlight, the color of the reaction mixture gradually changed to light brown, and stabilized to a dark brown solution after 15 min, indicating the completion of nucleation and the formation of Si-AgNPs (Figure 1). The color change of the reaction mixture from light yellow to dark brown is associated with the reduction of Ag^+ to AgNPs, which is facilitated by the biomolecules present in the plant extract [15,32]. Besides the visual examination, the formation of Si-AgNPs was validated by the absorption spectrum of Si-AgNPs obtained by the UV-Vis spectrophotometer. The UV-absorption spectrum of Si-AgNPs exhibited a peak at ~439 nm, which corresponded to the surface plasmon band (Figure 2). It is a well-known fact that the SPR band arises from the conduction of freely vibrating electrons in resonance with the incoming photons of light waves [33,34]. Very similar to the present findings, the absorption spectrum of AgNPs synthesized from Si leaf extracts showed an SPR peak at 426 nm and the reduction and capping of NPs was attributed to the plant bioactive compounds [26]. Recently, another study reported quick synthesis of AgNPs synthesized from mace arils [30].

Various researchers have proposed the possible mechanisms of sunlight-driven NP synthesis in earlier studies [35–37]. Some previous studies have shown the potential role of different intensities of visible light and the effect of UV-light in the electromagnetic spectrum on the synthesis of NPs [38–40]. A very quick and stable green synthesis of

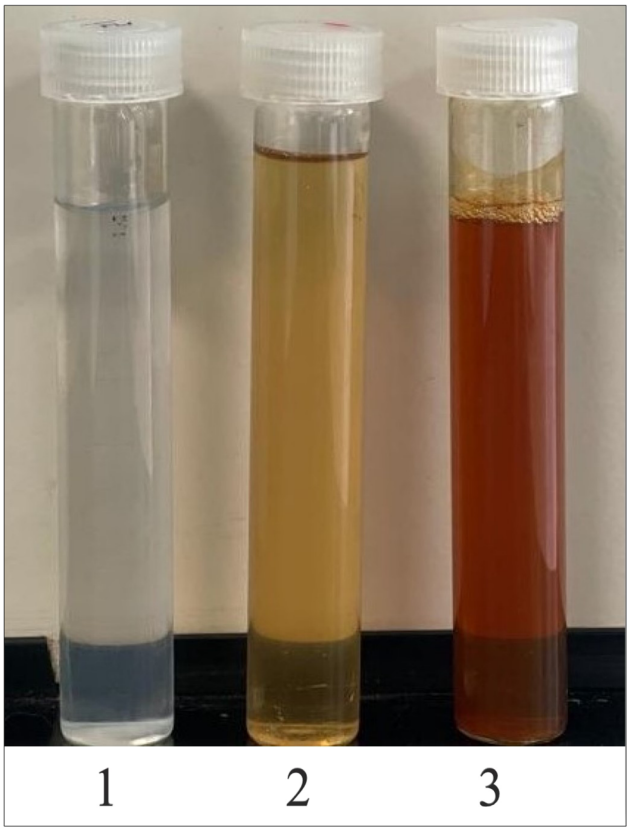

Figure 1: The formation of Si-AgNPs is indicated by color change. (1) $AgNO_3$: silver nitrate solution, (2) Si-extract: aqueous seed extract of *Sisymbrium irio*, and (3) Si-AgNPs: a dark brown colloidal mixture of green synthesized silver nanoparticles.

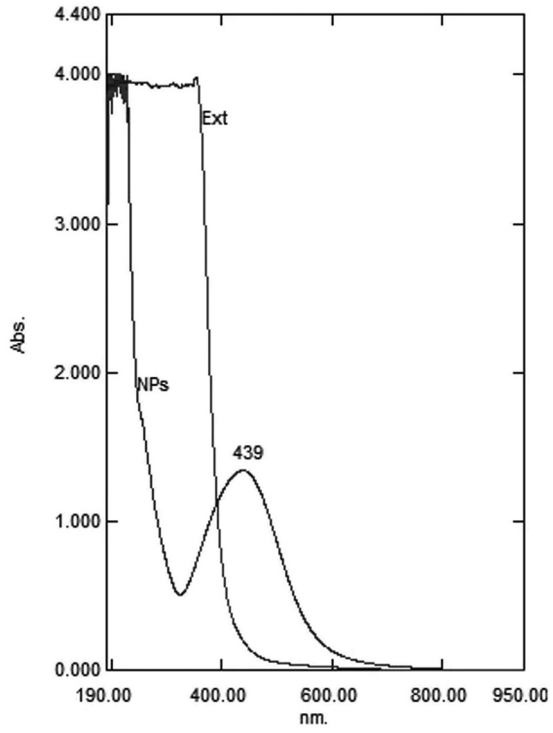

Figure 2: UV-Vis spectra of the synthesized Si-AgNPs, showing a broad absorption peak at ~439 nm and the Si seed extract.

AgNP was recently documented, and the synthesis was attributed to UV light [41]. However, another study showed that blue light, followed by red, green, and yellow light, was very effective in the synthesis of NPs, when used in the form of light filters [40]. In the present study, the rapid sunlight-mediated synthesis of Si-AgNPs took place in 15 min of direct exposure to sunlight. The reaction was carried out in glass containers. It is known that UV-light cannot pass through glass or plastic containers as its transmission is completely diminished [42–44]. Hence, the formation of Si-AgNPs could be due to the blue light of the visible spectrum, because it is suggested that blue light induces the release of hydrogen atoms due to tautomerization of some important biomolecules present in plant extracts, resulting in a reduction of Ag^+ ions [40,44,45].

3.2 TEM and DLS studies

The dimensions and arrangement of the synthesized Si-AgNPs were observed under a TEM (Figure 3). The TEM microphotographs illustrated that the Si-AgNPs were roughly spheroidal in shape and measured between 4 and 51 nm. Similar to our findings, TEM studies of NPs synthesized from leaves of Si showed small-sized spherical NPs in the range of 35–50 nm [26]. DLS analysis precisely provides the hydrodynamic diameter and size distribution of NPs. The average size of the Si-AgNPs was 94.81, and the polydiversity index (PDI) value was 0.270 (Figure 4). The low polydiversity index value and size distribution show that the particles are highly dispersed. DLS is an important technique that determines the hydrodynamic measurements of the NPs in association with biological molecules and ions attached to the NPs. The dimensions of Si-AgNPs as evidenced in microphotographs (4–51 nm) were smaller than the DLS measurements (Z-size, 94.81). The discrepancy in the size of NPs between the DLS and TEM findings is because the DLS technique measures the diameter of the synthesized nanoparticles in an aqueous medium, while the TEM measures them in a dry state, and the hydrodynamic measurements are always greater than the actual measurements [46]. It was reported earlier that the Brownian movement influences the size of NPs as these particles are distributed in a liquid medium [47]. Additionally, the hydrodynamic diameter is also influtenced by the covering of bioactive compounds present in the plant extract, which forms a coating around the NPs [48].

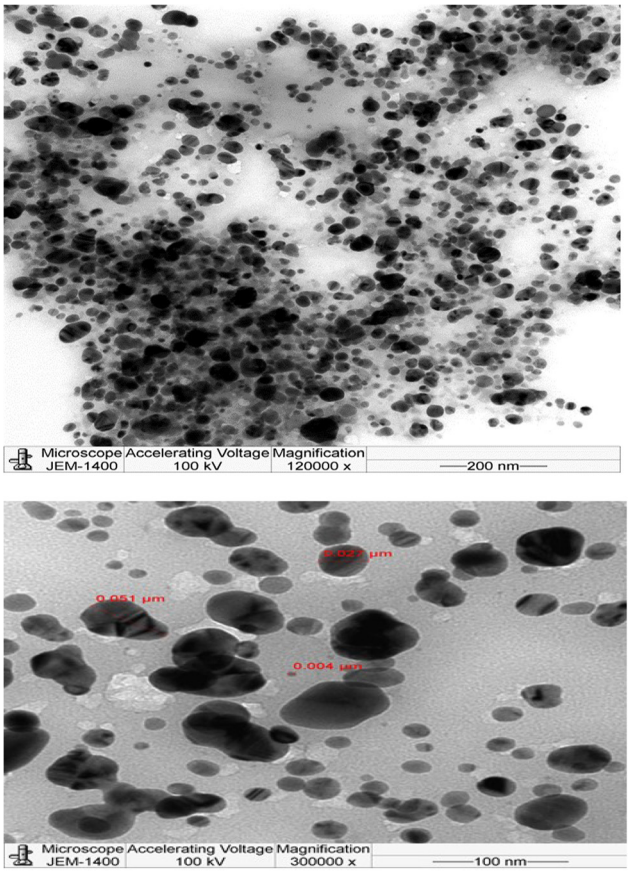

Figure 3: Transmission electron microphotograph showing the morphology and size of synthesized Si-AgNPs.

Our findings suggest that the Si-AgNPs were widely dispersed in the aqueous medium. These findings are consistent with those in a previous report [30].

3.3 Elemental analysis using EDX

The EDX elemental analysis spectrum of Si-AgNPs revealed an intense signal and an absorption peak at about 3 keV, which is typical of silver nanoparticles (Figure 5a). The silver content of the Si-AgNPs was nearly 68.3% as displayed in the EDX spectrum, indicating that silver was the dominant element. Aluminum (3.3%), sulfur (7.4%), potassium (7.4%), zinc (8%), and chlorine (3.4%) also showed signals in the spectrum (Figure 5b). These signals could be associated with various bioactive secondary metabolites and compounds present in the plant extract. The unique silver signal at 3 keV, evidenced in the spectrum, arises from SPR [49]. The EDX spectrum also displayed small silver peaks between 2.6 and 3.4 keV. The optical absorption peaks that are present between 2.5 and 4 keV are denoted by the absorption of metallic AgNPs [50]. Previous findings are in agreement with our results [51]. The distinct signals of elements (Cl, S, Al, Zn, and K) observed on the EDX spectrum in the present study might have resulted from the adsorption of various plant elements present in the seed extract that become bound to the surface of AgNPs during

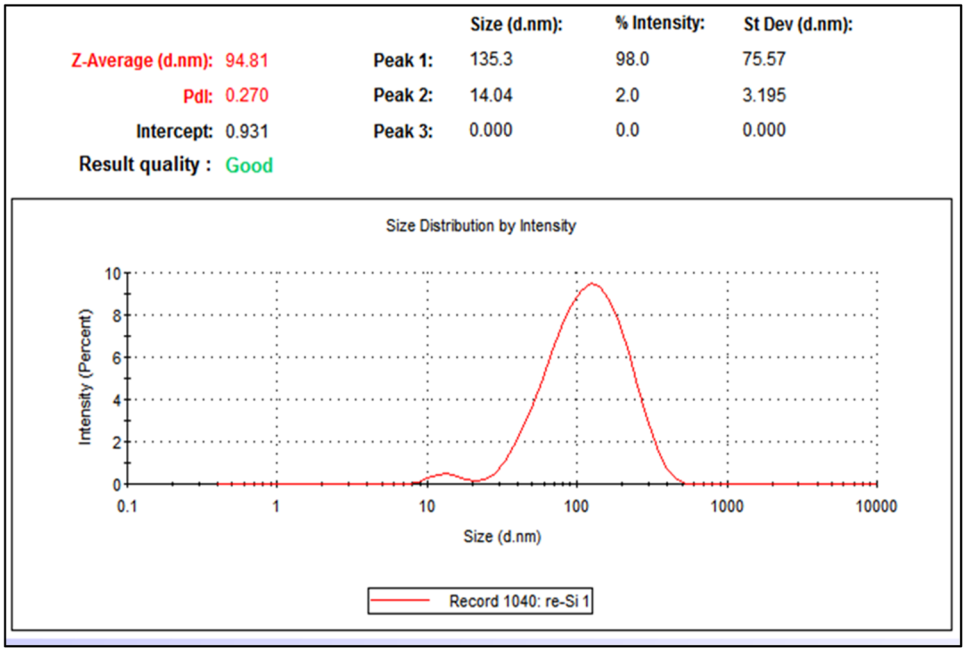

Figure 4: DLS spectrum showing the average hydro-dynamic size of synthesized Si-AgNPs.

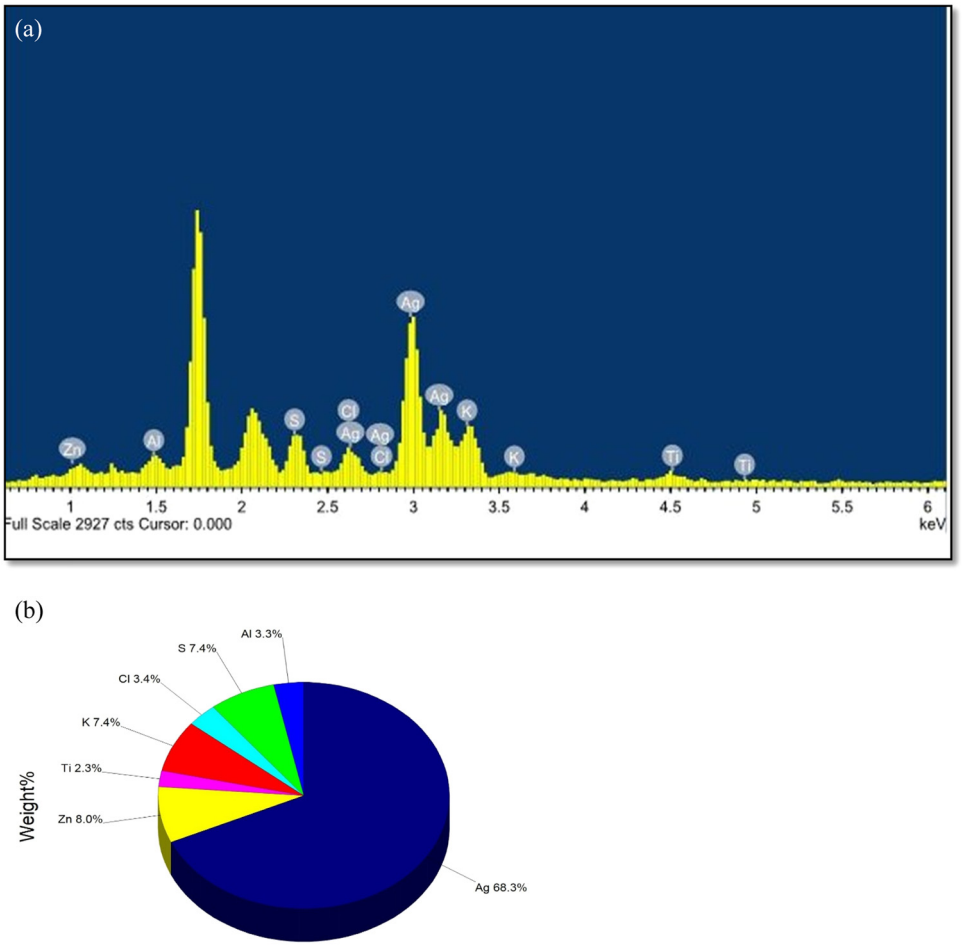

Figure 5: EDX spectrum of the green synthesized Si-AgNPs synthesized from the seeds of *S. irio*: (a) EDX spectrum showing the characteristic silver peak at 3 keV and (b) the elemental composition of Si-AgNPs.

synthesis. Similar findings in the EDX spectrum have been stated in previous research works [30,52].

3.4 FTIR analysis of aqueous seed extract of Si and Si-AgNPs

The spectra obtained from FTIR analysis of Si aqueous seed extract and synthesized Si-AgNPs are illustrated in Figure 6. The FTIR spectrum of seed extract revealed a clear broad peak of O–H stretching vibration at 3,432 cm^{-1}. This band could be attributed to alcoholic or phenolic compounds. A sharp peak with weak intensity at 2,929 cm^{-1} could be denoted to the (asymmetric) stretching vibration of the alkane (C–H bond). A typical peak characteristic of the amino group was observed at 1,653 cm^{-1}. The peaks at 1,518 and 1,423 cm^{-1} are due to the amide (in proteins) and aromatic C=C stretch. The peak at 1,274 cm^{-1} arose from the C–O stretch (aromatic esters), and the asymmetric stretch of C–O–C gave rise to the peak at 1,053 cm^{-1} (Figure 6). Similar to seed extracts, various peaks were also found in the IR spectrum of Si-AgNPs (Figure 6, NPs). However, the FTIR spectrum of Si-AgNPs showed some variations from the IR spectrum of seed extract. Among the few obvious changes observed in the Si-AgNPs spectrum were a shift in peak positions (3,432–3,425 and 2,929–2,931 cm^{-1}) and the appearance of a new medium- broad peak at 1,378 cm^{-1}, corresponding the OH bending of alcohols or phenols. A sharp peak at 1,052 cm^{-1} indicates asymmetric stretching of C–O–C. Three peaks, which were present in the IR spectrum of the seed extract at 1,518, 1,423, and 1,274 cm^{-1}, were missing from the Si-AgNPs spectrum. The peaks observed between 875 and 577 cm^{-1} in both the IR spectrum of extracts and synthesized nanoparticles of Si could be due to the strong C–Cl and C–I stretching of the halo compound.

The FTIR spectrum of seed extract and Si-AgNPs showed several peaks assigned to important functional groups, indicating the presence of bioactive compounds like amines, phenols, alcohols, saponins, carboxylic acids,

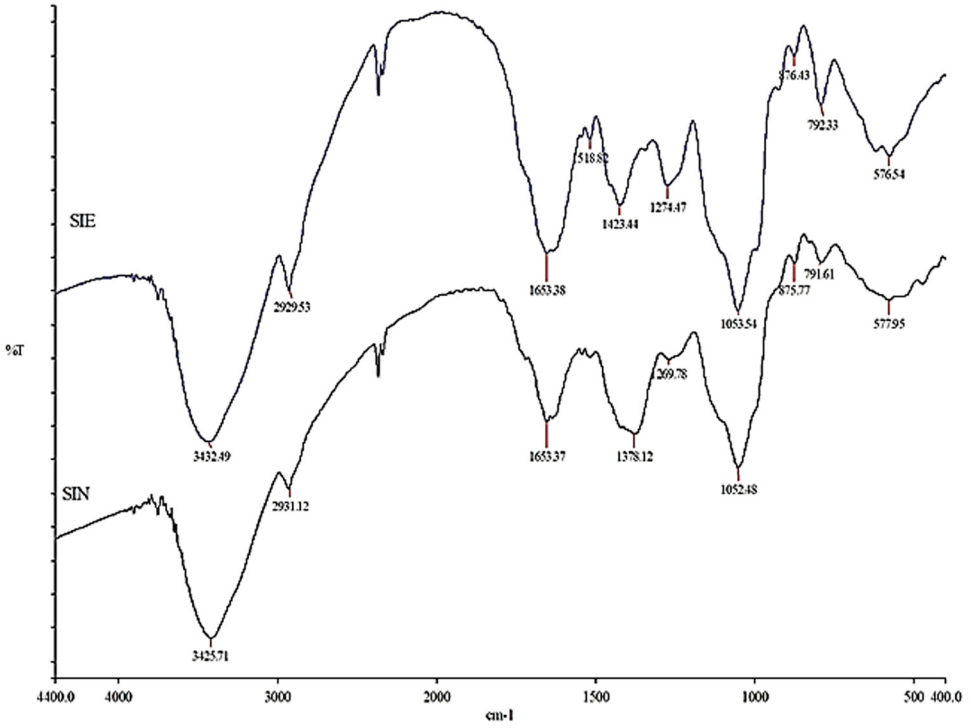

Figure 6: Fourier-transform infrared spectrum of the *Sisymbrium irio* seed extract and synthesized Si-AgNPs.

flavonoids, coumarins, alkaloids, tannins, and esters [22,53,54]. In agreement with the present findings, the FTIR spectrum of leaf extract and synthesized AgNPs showed peaks that were denoted to alcohols, phenols, amino acids, coumarins, triterpenes, flavonoids, and glycosides [26]. Ten flavonoids were isolated and identified from the aerial parts of Si, grown in Saudi Arabia [22]. Yet in another study, Al Massrani et al. isolated three important phytosterols (stigmasterol, b-sitosterol, and b-sitosterol-b-D-glucoside) from the aerial parts of Si grown in Saudi Arabia [54]. Similarly, quercetin, sitosterol, isorhamnetin, and β-sitosteryl-D-glucoside were isolated in earlier studies [55]. The phytochemical analysis of various organic extracts of different parts of the Si plant, growing in Saudi Arabia, exhibited the presence of several important biochemical compounds that included steroids, phenols, flavonoids, glycosides, triterpenoids, isothiocyanates, tannins, carbohydrates, alkaloids, and saponins [53]. Biomolecules and secondary metabolites present in plant extracts act as reductants, facilitating capping and conferring stability to NPs [50]. The new peak at 1,378 cm^{-1} in the FTIR spectrum of Si-AgNPs corresponds to the carbonyl group (C═O stretching) and it is associated with the reduction of Ag^{+} ions to AgNPs [56,57]. The disappearance of a few peaks (1,518, 1,423, and 1,274 cm^{-1}) in the FTIR spectrum of Si extract indicates encapsulation of NPs by amino and polyphenolic compounds [30]. Furthermore, certain bioactive compounds (phenols, alcohols, amines, and proteins) present in plant extracts can bind readily to silver and form a layer around it, conferring stability, preventing agglomeration, and thus helping with capping [58,59]. These results are in agreement and corelate with a previous report which showed the presence of the functional groups reported in the leaf extract and synthesized nanoparticles of Si [26,53].

3.5 Effect of Si-AgNPs on mycelial growth and spore germination of some fungal plant pathogens

The antifungal activity of Si-AgNPs has been demonstrated in the Figures 7–9. All the fungal isolates showed growth inhibition when treated with Si-AgNPs, except for *Trichoderma harzianum* (Figure 7). At 80 $\mu g \cdot mL^{-1}$, the Si-AgNPs inhibited *Alternaria alternata* with the smallest colony diameter of 1.36 cm, followed by *F. oxysporum* (2.3 cm), *F. solani* (3.10 cm), and *A. brassicae* (4.50 cm) (Figure 8). Similarly, at 80 $\mu g \cdot mL^{-1}$, the highest percentage of mycelial growth inhibition was shown by *A. alternaria* (83%), followed by *Fusarium oxysporum* (71%), and

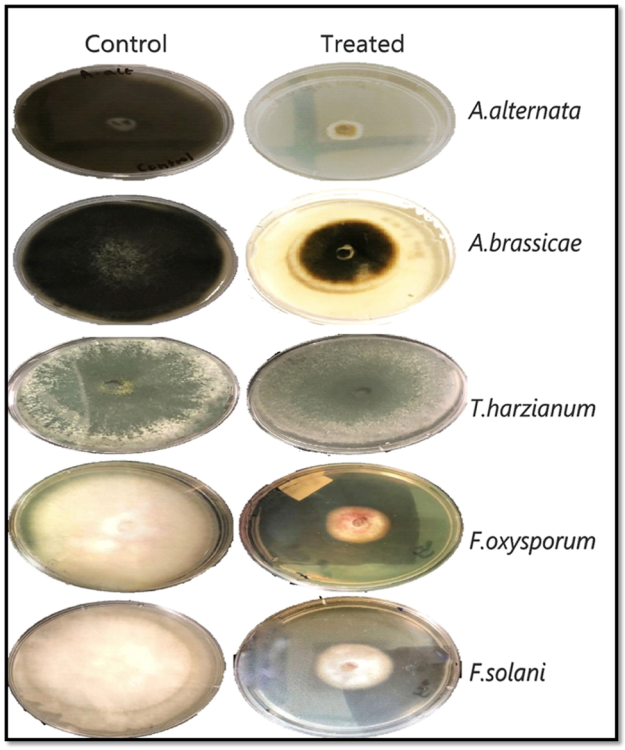

Figure 7: Antifungal activity of Si-AgNPs against plant pathogenic fungi at 80 µg·mL^{-1}.

F. solani (61%). However, among all the test isolates, *A. brassicae* exhibited moderate growth inhibition (Figure 9). All the test isolates were inhibited by $AgNO_3$, but the inhibition was quite negligible in comparison to Si-AgNPs (Figures 8 and 9). Strong inhibitory effects on mycelial growth were witnessed when the test fungi were treated with the fungicide carbendazim. The green synthesized Si-AgNPs showed remarkable spore inhibitory activity as well. As the concentration of Si-AgNPs increased, the spore germination rate decreased. In fact, at the highest test concentration of 80 µg·mL^{-1} the spore germination decreased to 7% in *A. alternata* and 15% in *F. oxysporum*. Distilled water, which served as a negative control, did not have any inhibitory activity on spore germination, while the positive control, carbendazim, showed strong inhibition on spore germination (Figure 10).

Except for *T. harzianum*, all the test isolates used in this study showed significant growth inhibition when treated with Si-AgNPs, indicating the potent effect of Si-AgNPs in controlling fungal mycelial growth. Though the exact mechanism of antifungal activity is still unclear, a recent research report has documented that AgNPs can make direct contact with the cell wall. The NPs then penetrate the cell membrane and disrupt the cell integrity [60]. According to another viewpoint, AgNPs can easily

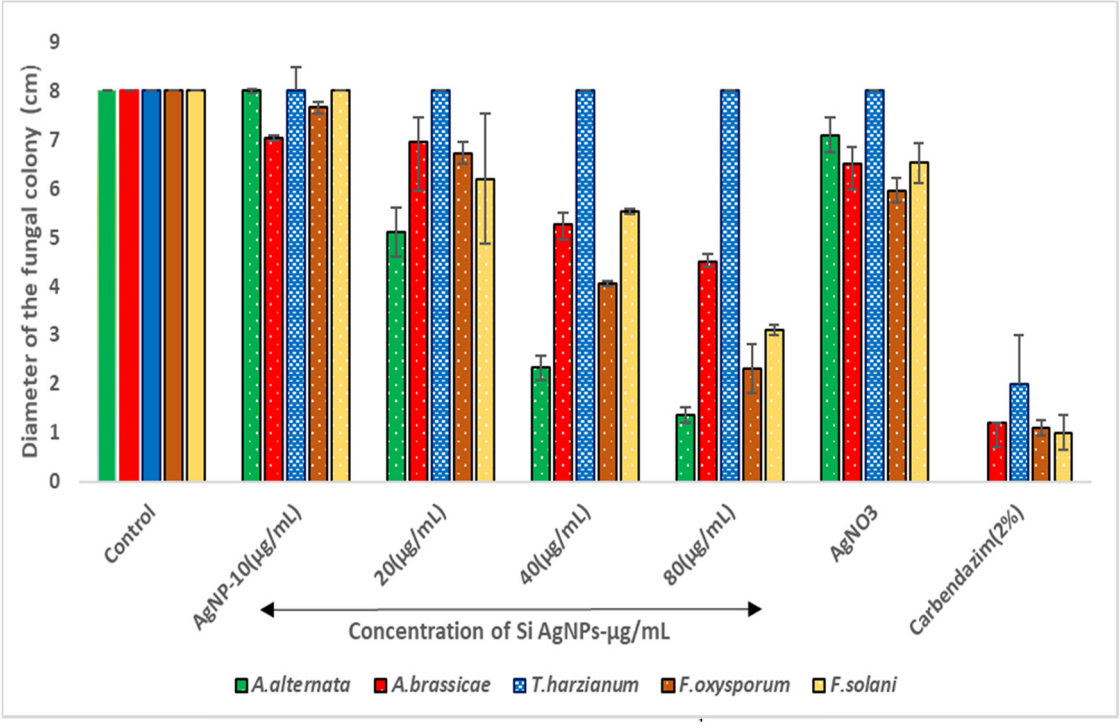

Figure 8: The effect of various concentrations (10–80 µg·mL^{-1}) of Si-AgNPs on the mycelial growth of phytopathogenic fungi.

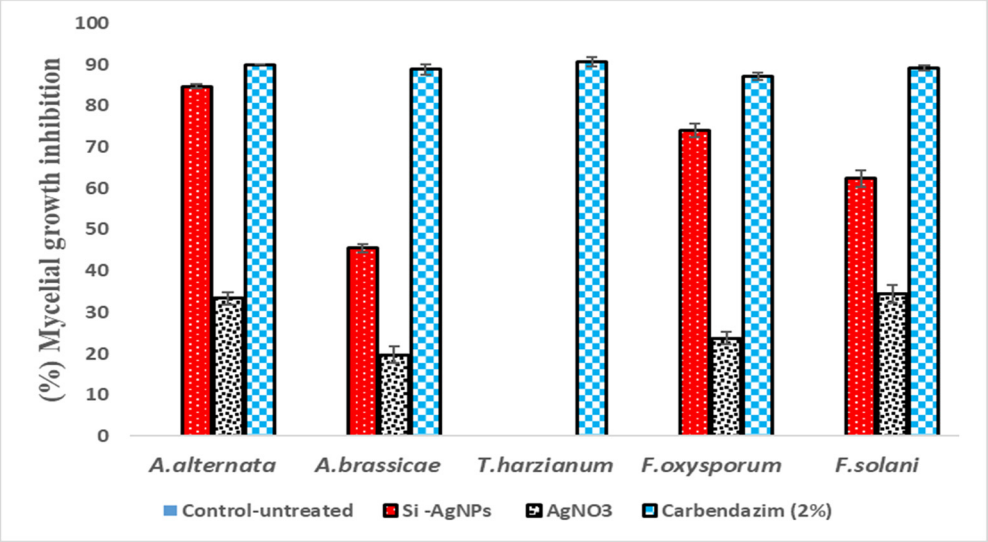

Figure 9: Percentage mycelial growth inhibition of fungal isolates treated with Si-AgNPs at 80 µg·mL^{-1}.

permeate the cell wall, accumulate in the cell membrane, and then interfere with ergosterol synthesis and disrupt its functioning due to their small size. All the aforementioned events result in altered permeability and osmotic imbalance, resulting in cell death [61–63]. Some reports suggest that once the AgNPs enter the fungal cell cytoplasm, the NPs cause damage to DNA, RNA, and cellular proteins, resulting in enhanced production of reactive oxygen species (ROS) [64–66]. Leakage of cellular content ultimately leads to cell death [65,66]. The poor antifungal activity exhibited by Si-AgNPs and plant extract against *T. harzianum* could be due to the inability of the AgNPs to make direct contact with the cell wall or failure to permeate the cell membrane. Previous reports have shown that resistance to antimicrobial drugs and NPs is attributed to multiple factors [67–69]. The possible mechanisms could be decreased permeability of the cell membrane or altered activity of efflux pumps [67,68]. In agreement with our findings, previous studies have shown poor mycelial growth inhibition of *Pestalotiopsis mangiferae* in comparison to other fungal isolates when treated with red currant extracts and synthesized nanoparticles [70].

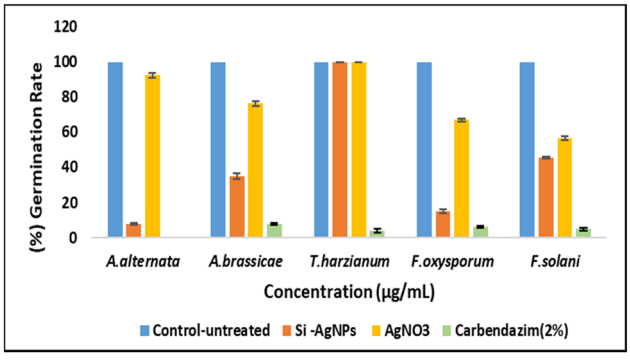

Figure 10: The effect of the biosynthesized Si-AgNPs on spore germination of fungal test isolates at 80 µg·mL^{-1}.

Fungal spores are vital in the establishment and spread of infection in plants, as they germinate and increase colonization through mycelial growth [52]. In this study, Si-AgNPs significantly reduced spore germination of the test fungi. Similarly, other studies have reported that an increase in the concentration of the biosynthesized AgNPs had a stronger inhibitory effect on hyphal growth and conidial germination [27,71]. Overall, the potent spore and mycelial inhibition observed in the present study could be credited to the synergy of bioactive molecules present in the seed extracts and the micro size of the Si-AgNPs, which created a perfect combination that could target the fungal cell destruction effectively. Previous reports are in agreement with our present findings, as they have demonstrated the potent antimicrobial activity of green synthesized NPs against a number of pathogenic fungi and bacteria [15,25,27,30,52]. It is reported that the disturbed metabolic functions and cellular damage caused by AgNPs stimulate the oxidative stress which inhibits spore germination and mycelial growth also leading to cell death [61,65].

3.6 Cytotoxicity of Si-AgNPs against HeLA cell lines

The cytotoxicity studies with two-fold serial dilution of Si-AgNPs against the HeLa cervical cancer cell line showed

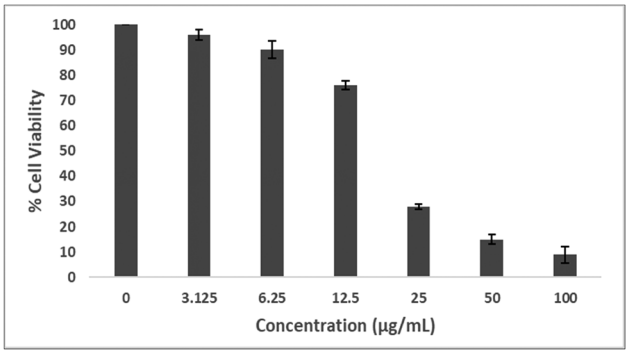

Figure 11: Cytotoxicity of green synthesized Si-AgNPs using aqueous seed extracts evaluated against cervical cancer cell lines (HeLa cell line).

significant cytotoxic activity. Figure 11 depicts that as the concentration of the NPs increased, the number of viable cells decreased, with an IC_{50} value of 22.06 ± 0.86 µg·mL^{-1}. However, lower concentrations (3.125 and 6.25 µg·mL^{-1}) demonstrated poor activity against cancer cells. A previous report showed significant dose-dependent cytotoxicity activity of a purified fraction from hexane extracts of *Sisymbrium irio* aerial parts against Vero cancer cell lines [72].

Sisymbrium irio is bestowed with numerous bioactive compounds, which include phenols, flavonoids, amines, steroids, coumarins, glycosides, indoles, and isothiocyanates [22,23,54]. Previous studies have shown that consumption of vegetables belonging to the Cruciferae family reduces the risk of colorectal and lung cancer [73,74]. This cancer-preventive property of Cruciferae members was associated with a synergistic effect of the numerous chemical compounds and the beneficial nutrients present in the edible parts of the plants [75]. Glucosinolates are an important sulfur compound present in cruciferous vegetables [76]. Upon hydrolysis, glucosinolates breakdown into isothiocyanates and indoles. Previous research has shown that both the aforementioned compounds are cancer-preventive and chemoprotective [77,78]. Preliminary human studies on a small group of individuals have shown that consumption of indole-3-carbinol (I3C) as a supplement may be advantageous in treating cancers like recurrent respiratory papillomatosis and human papilloma virus infection, for example, cervical intraepithelial neoplasia [79].

Hence, the noteworthy cytotoxic activity shown by Si-AgNPs could be due to chemical compounds present in the aerial parts of the Si plant and the NPs together. The secondary metabolites present in the seeds of Si like phenols, indoles, isothiocyanates, flavonoids, and amino compounds could have formed a covering around AgNPs and caused the robust cytotoxic activity. The NP entry alters cell permeability. Once inside the cells, NPs create an upheaval by interacting with mitochondria and DNA, inhibiting transcription and vital synthesis processes, which results in an increase in ROS and oxidative stress, ultimately leading to cell death from toxicity [80–82]. The findings of this study are in perfect concurrence with previous studies which have shown the dose-dependent cytotoxic activity of AgNPs synthesized from plants against several cancer cell lines, including the HeLa cell line [83–85]. Hence, the antimicrobial and cytotoxic activity of Si-AgNPs could be designated to the colligative effect of biomolecules with AgNPs, resulting in altered cell membrane permeability, which leads to several destructive changes leading to cell death.

4 Conclusion

Every year, plant pathogens cause significant damage to plants and their products. Several methods are used to control their growth, all of which have detrimental effects on humans and the environment. As a result, current circumstances necessitate the use of risk-free and environmentally friendly control methods. Green synthesized AgNPs are an excellent alternative that is environmentally friendly, effective, widely available, and affordable for everyone. In the current study, biosynthesized AgNPs from the seed extracts of Si caused noticeable fungistatic properties against the selected plant pathogenic fungi. With the highest test concentration, there was significant *in vitro* mycelial inhibition and a reduction in spore germination. Similarly, Si-AgNPs demonstrated significant cytotoxic activity against HeLa cells, indicating their potential as anticancer studies. However, further studies to understand their toxicity towards cells and their mode of action are required.

Acknowledgement: The authors would like to extend their sincere appreciation to the Research Supporting Project (number: RSP-2021/229), King Saud University, Riyadh, Saudi Arabia. for payment of the charge for publishing this manuscript.

Funding information: This research project was supported by a grant from the Research Supporting Project (number RSP-2021/229), King Saud University, Riyadh, Saudi Arabia.

Author contributions: Humaira Rizwana: concept and design of the study, project administration, writing – original draft, and writing – review and editing; Najat A. Bokahri:

methodology, resources, funding acquisition, and project administration; Ahmed Alfarhan: writing – review and editing, statistical analysis, and validation; Horiah A. Aldehaish: methodology, experimental work, resources, and data collection; Noura S. Alsaggabi: formal analysis of the results and compilation.

Conflict of interest: Authors state no conflict of interest

References

[1] Chaturvedi S, Dave PN. Chapter 59 – Nanomaterials: environmental, human health risk. In: Hussain CM, editor. Micro and nano technologies, handbook of nanomaterials for industrial applications. Cambridge, MA: Elsevier; 2018. p. 1055–62. doi: 10.1016/B978-0-12-813351-4.00061-4.

[2] Roy A, Bulut O, Some S, Mandal AK, Yilmaz MD. Green synthesis of silver nanoparticles: biomolecule-nanoparticle organizations targeting antimicrobial activity. RSC Adv. 2019;9:2673–702. doi: 10.1039/C8RA08982E.

[3] Lyddy R. Chapter 36 – Nanotechnology. In: Wexler P, Gilbert SG, Hakkinen PJ, Mohapatra A, editors. Information resources in toxicology. 4th edn. Academic Press; 2009. p. 321–8. doi: 10.1016/B978-0-12-373593-5.00036-7.

[4] Khare S, Williams K, Gokulan K. Nanotechnology. In: Batt CA, Tortorello ML, editors. Encyclopedia of food microbiology. 2nd edn. Academic Press; 2014. p. 893–900. ISBN 9780123847331. doi: 10.1016/B978-0-12-384730-0.00406-7.

[5] Singh R, Hano C, Nath G, Sharma B. Green biosynthesis of silver nanoparticles using leaf extract of carissa carandas L. and their antioxidant and antimicrobial activity against human pathogenic bacteria. Biomolecules. 2021;11:299. doi: 10.3390/biom11020299.

[6] Parfitt J, Barthel M, Macnaughton S. Food waste within food supply chains: quantification and potential for change to 2050. Philos Trans R Soc Lond B Biol Sci. 2010;365:3065–81. doi: 10.1098/rstb.2010.0126.

[7] Díaz-Dellavalle P, Cabrera A, Alem D, Larrañaga P, Ferreira F, Dalla M. Research: antifungal activity of medicinal plant extracts against phytopathogenic fungus alternaria spp. Chil J Agr Res. 2011;71:231–9. doi: 10.4067/S0717-97072019000204459.

[8] FAO. The state of food and agriculture 2019. Moving forward on food loss and waste reduction. Rome: FAO; 2019. Licence: CC BY-NC-SA 3.0 IGO.

[9] Özkara A, Akyıl D, Konuk M. In: Larramendy ML, Soloneski S, editors. Pesticides, environmental pollution, and health, environmental health risk – hazardous factors to living species. Intech Open; 2016. doi: 10.5772/63094. Available from: https://www.intechopen.com/chapters/50482.

[10] Dauthal P, Mukhopadhyay M. Biosynthesis of palladium nanoparticles using *Delonix regia* leaf extract and its catalytic activity for nitro-aromatics hydrogenation. Ind Eng Chem Res. 2013;52(51):18131–9. doi: 10.1021%2Fie403410z.

[11] Abomuti MA, Danish EY, Firoz A, Hasan N, Malik MA. Green synthesis of zinc oxide nanoparticles using salvia officinalis leaf extract and their photocatalytic and antifungal activities. Biology (Basel). 2021;10(11):1075. doi: 10.3390/biology10111075.

[12] Doan Thi TU, Nguyen TT, Thi YD, Ta Thi KH, Phan BT, Pham KN. Green synthesis of ZnO nanoparticles using orange fruit peel extract for antibacterial activities. RSC Adv. 2020;10:23899–907. doi: 10.1039/d0ra04926c.

[13] Shabaani M, Rahaiee S, Zare M, Jafari SM. Green synthesis of ZnO nanoparticles using loquat seed extract; Biological functions and photocatalytic degradation properties. LWT. 2020;13:110133. doi: 10.1016/j.lwt.2020.110133.

[14] Abdallah Y, Ogunyemi SO, Abdelazez A, Zhang M, Hong X, Ibrahim E, et al. The green synthesis of MgO nano-flowers using rosmarinus officinalis L. (Rosemary) and the antibacterial activities against *Xanthomonas oryzae pv. oryzae*. BioMed Res Int. 2019;8, Article ID 5620989. doi: 10.1155/2019/5620989.

[15] Rizwana H, Alwhibi MS, Aldarsone HA, Awad MA, Soliman DA, Bhat RS. Green synthesis, characterization, and antimicrobial activity of silver nanoparticles prepared using *Trigonella foenum-graecum* L. leaves grown in Saudi Arabia. Green Process Synth. 2021;10:421–9.

[16] Niraimathee VA, Subha V, Ravindran RE, Renganathan S. Green synthesis of iron oxide nanoparticles from *Mimosa pudica* root extract. Int J Environ Sustain Dev. 2016;15:227.

[17] Keat CL, Aziz A, Eid AM, Elmarzugi NA. Biosynthesis of nanoparticles and silver nanoparticles. Bioresour Bioprocess. 2015;2:47. doi: 10.1186/s40643-015-0076-2.

[18] Khan AA, Alanazi AM, Alsaif NF, Wani TA, Bhat MA. Pomegranate peel induced biogenic synthesis of silver nanoparticles and their multifaceted potential against intracellular pathogen and cancer. Saudi J Biol Sci. 2021;28:4191–200. doi: 10.1016/j.sjbs.2021.06.022.

[19] Alsubki R, Tabassum H, Abudawood M, Rabaan AA, Alsobaie SF, Ansar S. Green synthesis, characterization, enhanced functionality and biological evaluation of silver nanoparticles based on *Coriander sativum*. Saudi J Biol Sci. 2021;28(4):2102–8. doi: 10.1016/j.sjbs.2020.12.055.

[20] Collenete S. Wild flowers Saudi Arabia, Nick Lear. U.K: East Anglvan Engroving Co. Ltd.; 1999. p. 123.

[21] Bolus L. Medicinal plant of North Africa, Reference Publications Inc: chemical constituents of *Sisymbrium irio* L. from Jordan. Nat Prod Res. 1983;24(5):448–56.

[22] Al-Jaber NA. Phytochemical and biological studies of *Sisymbrium irio* L. growing in Saudi Arabia. J Saudi Chem Soc. 2011;15(4):345–50. doi: 10.1016/j.jscs.2011.04.010.

[23] Vohora SB, Naqvi SA, Kumar I. Antipyretic, analgesic and antimicrobial studies on *Sisymbrium irio*. Planta Med. 1980;38:255–9. doi: 10.1055/s-2008-1074870.

[24] Qidwai A, Kumar R, Dikshit A. Green synthesis of silver nanoparticles by seed of *Phoenix sylvestris* L. and their role in the management of cosmetics embarrassment. Green Chem Lett Rev. 2018;11(2):176–88. doi: 10.1080/17518253.2018.1445301.

[25] Nguyen DH, Lee JS, Park KD, Ching YC, Nguyen XT, Phan VHG, et al. Green silver nanoparticles formed by phyllanthus urinaria, pouzolzia zeylanica, and scoparia dulcis leaf extracts and the antifungal activity. Nanomaterials. 2020;10:542. doi: 10.3390/nano10030542.

[26] Mickymaray S. One-step synthesis of silver nanoparticles using Saudi Arabian desert seasonal plant *Sisymbrium irio*

and antibacterial activity against multidrug-resistant bacterial strains. Biomolecules. 2019;9:662. doi: 10.3390/biom9110662.

[27] Ibrahim E, Luo J, Ahmed T, Wu W, Yan C, Li B. Biosynthesis of silver nanoparticles using onion endophytic bacterium and its antifungal activity against rice pathogen *Magnaporthe oryzae*. J Fungi (Basel).2020;6:294. doi: 10.3390/jof6040294.

[28] Rizwana H. Postharvest control of anthracnose lesions and its causative agent, *Colletotrichum musae* by some oils. Cell Mol Biol (Noisy-Le-Grand). 2018;64:52–8. doi: 10.14715/cmb/2018.64.4.9. PMID: 29641375.

[29] Xing K, Liu Y, Shen X, Zhu X, Li X, Miao X, et al. Effect of O-chitosan nanoparticles on the development and membrane permeability of *Verticillium dahliae*. Carbohydr Polym. 2017;165:334–43. doi: 10.1016/j.carbpol.2017.02.063.

[30] Rizwana H, Bokahri NA, Alkhattaf FS, Albasher G, Aldehaish HA. Antifungal, antibacterial, and cytotoxic activities of silver nanoparticles synthesized from aqueous extracts of mace-arils of *Myristica fragrans*. Molecules. 2021;26(24):7709. doi: 10.3390/molecules26247709.

[31] Gomha SM, Riyadh SM, Mahmmoud EA, Elaasser MM. Synthesis and anticancer activities of thiazoles,1,3-thiazines, and thiazolidine using chitosan-grafted-poly (vinylpyridine) as basic c catalyst. Heterocycles. 2015;91:1227–43.

[32] Ahmad A, Mukherjee P, Senapati S, Mandal D, Khan MI, Kumar R, et al. Extracellular biosynthesis of silver nanoparticles using the fungus *Fusarium oxysporum*. Colloids Surf B Biointerfaces. 2003;28(4):313–8.

[33] Singh J, Dutta T, Kim KH, Rawat M, Samddar P, Kumar P. 'Green' synthesis of metals and their oxide nanoparticles: applications for environmental remediation. J Nano Biotechnol. 2018;16:84. doi: 10.1186/s12951-018-0408-4.

[34] Csaki A, Stranik O, Fritzsche W. Localized surface plasmon resonance based biosensing. Expert Rev Mol Diag. 2018;18:279–96. doi: 10.1080/14737159.2018.1440208.

[35] Rawat V, Sharma A, Bhatt VP, Singh RP, Maurya IK. Sunlight mediated green synthesis of silver nanoparticles using *Polygonatum graminifolium* leaf extract and their antibacterial activity. Mater Today Proc. 2020;29:911–6. doi: 10.1016/j.matpr.2020.05.274.

[36] Bernabo M, Pucci A, Galembeck A, Leite CADP, Ruggeri G. Thermal and sun promoted generation of silver nanoparticles embedded into poly(vinyl alcohol) films. Macromol Mater Eng. 2009;294:256–64.

[37] Sooraj MP, Nair AS, Vineetha D. Sunlight-mediated green synthesis of silver nanoparticles using Sida retusa leaf extract and assessment of its antimicrobial and catalytic activities. Chem Pap. 2021;75:351–63.

[38] Mallick K, Witcomb MJ, Scurrell MS. Polymer stabilized silver nanoparticles: a photochemical synthesis route. J Mate Sci. 2004;39:4459–63.

[39] Mallick K, Witcomb MJ, Scurrell MS. Silver nanoparticle catalysed redox reaction: an electron relay effect. Mater Chem Phys. 2006;97:283–7.

[40] Yang N, Wei X, Li W. Sunlight irradiation induced green synthesis of silver nanoparticles using peach gum polysaccharide and colorimetric sensing of H_2O_2. Mater Lett. 2015;154:21–4. doi: 10.1016/J.MATLET.2015.03.034.

[41] Prathna TC, Raichur AM, Chandrasekaran N, Mukherjee A. Sunlight irradiation induced green synthesis of stable silver nanoparticles using *Citrus limon* extract. Proc Natl Acad Sci India Sect B Biol Sci. 2013;84:65–70. doi: 10.1007/s40011-013-0193-7.

[42] Mathew S, Prakash A, Radhakrishnan EK. Sunlight mediated rapid synthesis of small size range silver nanoparticles using *Zingiber officinale* rhizome extract and its antibacterial activity analysis. Inorg Nano Met Chem. 2018;48:139–45.

[43] Nguyen VT. Sunlight-driven synthesis of silver nanoparticles using Pomelo peel extract and antibacterial testing. J Chem. 2020;6407081:9. doi: 10.1155/2020/6407081.

[44] Jayapriya MG, Dhanasekaran D, Arulmozhi M, Nandhakumar E, Senthilkumar N, Sureshkumar K. Green synthesis of silver nanoparticles using *Piper longum* catkin extract irradiated by sunlight: ANTIBACTERIAL and catalytic activity. Res Chem Intermed. 2019;45:3617–31. doi: 10.1007/s11164-019-03812-5.

[45] Bhardwaj AK, Shukla A, Maurya S, Singh SC, Uttam KN, Sundaram S, et al. Direct sunlight enabled photo-biochemical synthesis of silver nanoparticles and their bactericidal efficacy: Photon energy as key for size and distribution control. J Photochem Photobiol B Biol. 2018;188:42–9. doi: 10.1016/j.jphotobiol.2018.08.019.

[46] Huang J, Li Q, Sun D, Lu Y, Su Y, Yang X, et al. Biosynthesis of silver and gold nanoparticles by novel sun dried *Cinnamomum camphora* leaf. Nanotechnol. 2007;18:105104. doi: 10.1088/0957-4484/18/10/105104.

[47] De Aragao AP, de Oliveira TM, Quelemes PV, Perfeito MLG, Araujo MC, Santiago JDAS, et al. Green synthesis of silver nanoparticles using the seaweed *Gracilaria birdiae* and their antibacterial activity. Arab J Chem. 2016;12:4182–8.

[48] Zhang XF, Liu ZG, Shen W, Gurunathan S. Silver nanoparticles: synthesis, characterization, properties, applications, and therapeutic approaches. Int J Mol Sci. 2016;17:1534.

[49] Kaviya S, Santhanalaksnmi J, Viswanathan B, Muthumany J, Srinivasan K. Biosynthesis of silver nanoparticles using *Citrus sinensis* peel extract and its antibacterial activity. Spectrochim Acta Part A. 2011;79:594–8. doi: 10.1016/j.saa.2011.03.040.

[50] Magudapathy P, Gangopadhyay P, Panigrahi BK, Nair KGM, Dhara S. Electrical transport studies of Ag nanoclusters embedded in glass matrix. Physica B: Condensed Matter. 2001;299:142–6. doi: 10.1016/S0921-4526(00)00580-9.

[51] Anandalakshmi K, Venugobal J, Ramasamy V. Characterization of silver nanoparticles by green synthesis method using *Pedalium murex* leaf extract and their antibacterial activity. Appl Nanosci. 2016;6:399–408. doi: 10.1007/s13204-015-0449-z.

[52] Rizwana H, Alwhibi MS. Biosynthesis of silver nanoparticles using leaves of *Mentha pulegium*, their characterization, and antifungal properties. Green Process Synth. 2021;10:824–34.

[53] Khalil HE, Aljeshi YM, Saleh FA. Phytochemical analysis and *in vitro* antioxidant properties of *Sisymbrium irio* L. growing in saudi arabia: a comparative study. RJPBCS. 2017;8(3):2533.

[54] Al-Massarani SM, El-Gamal AA, Alam P, Al-Sheddi ES, Al-Oqail MM, Farshori NN. Isolation, biological evaluation and validated HPTLC-quantification of the marker constituent of the edible Saudi plant *Sisymbrium irio.* L. Saudi Pharm J. 2017;25:750–9. doi: 10.1016/j.jsps.2016.10.012.

[55] Kahan M, Kalim S, Kahan M. Chemical constituents of the aerial parts of *Sisymbrium irio*. J Indian Chem Soc. 1991;68:532.

[56] Singh K, Panghal M, Kadyan S, Chaudhary U, Yadav JP. Antibacterial activity of synthesized silver nanoparticles from *Tinospora cordifolia* against multi drug resistant strains of *Pseudomonas aeruginosa* isolated from burn patients. J Nanomed Nanotechnol. 2014;5:192. doi: 10.4172/2157-7439.1000192.

[57] Anuj SA, Ishnava KB. Plant mediated synthesis of silver nanoparticles by using dried stem powder of *Tinospora cordifolia*, its antibacterial activity and comparison with antibiotics. Int J Pharma Biol Sci. 2013;4:849–63.

[58] Aslany S, Tafvizi F, Naseh V. Characterization and evaluation of cytotoxic and apoptotic effects of green synthesis of silver nanoparticles using *Artemisia Ciniformis* on human gastric adenocarcinoma. Mater Today Commun. 2020;24:101011.

[59] Sre PR, Reka M, Poovazhagi R, Kumar MA, Murugesan K. Antibacterial and cytotoxic effect of biologically synthesized silver nanoparticles using aqueous root extract of *Erythrina indica* lam. Spectrochim Acta Part A. 2015;135:1137–44.

[60] Mikhailova EO. Silver nanoparticles: mechanism of action and probable bio-application. J Funct Biomater. 2020;11:84. doi: 10.3390/jfb11040084.

[61] Kim KJ, Sung WS, Suh BK, Moon SK, Choi JS, Kim JG, et al. Antifungal activity and mode of action of silver nano-particles on *Candida albicans*. Biometals. 2009;22:235–42. doi: 10.1007/s10534-008-9159-2.

[62] Kim SW, Jung JH, Lamsal K, Kim YS, Min JS, Lee YS. Antifungal effects of silver nanoparticles (AgNPs) against various plant pathogenic fungi. Mycobiol. 2012;40:53e58.

[63] Berger TJ, Spadaro JA, Chapin SE, Becker RO. Electrically generated silver ions: quantitative effects on bacterial and mammalian cells. Antimicrob Agents Chemother. 1976;9(2):357–8. doi: 10.1128/AAC.9.2.357.

[64] Lara HH, Romero-Urbina DG, Pierce C, Lopez-Ribot JL, Arellano-Jiménez MJ, Jose-Yacaman M. Effect of silver nanoparticles on *Candida albicans* biofilms: an ultrastructural study. J Nanobiotechnol. 2015;13:91. doi: 10.1186/s12951-015-0147-8.

[65] Kumari M, Giri VP, Pandey S, Kumar M, Katiyar R, Nautiyal CS, et al. An insight into the mechanism of antifungal activity of biogenic nanoparticles than their chemical counterparts. Pest Biochem Physiol. 2019;157:45–52.

[66] Zhou L, Zhao X, Li M, Lu Y, Ai C, Jiang C, et al. Antifungal activity of silver nanoparticles synthesized by iturin against *Candida albicans in vitro* and *in vivo*. Appl Microbiol Biotechnol. 2021;1105:3759–70. doi: 10.1007/s00253-021-11296-w.

[67] Sanglard D. Emerging threats in antifungal-resistant fungal pathogens. Front Med (Lausanne). 2016;3:11.

[68] Salomoni R, Léo P, Montemor AF, Rinaldi BG, Rodrigues M. Antibacterial effect of silver nanoparticles in *Pseudomonas aeruginosa*. Nanotechnol Sci Appl. 2017;10:115–21.

[69] Vandeputte P, Ferrari S, Coste AT. Antifungal resistance and new strategies to control fungal infections. Int J Microbiol. 2012;3:713687. doi: 10.1155/2012/713687.

[70] Rizwana H, Alwhibi MS, Al-Judaie RA, Aldehaish HA, Alsaggabi NS. Sunlight-mediated green synthesis of silver nanoparticles using the berries of *Ribes rubrum* (red currants): characterisation and evaluation of their antifungal and antibacterial activities. Molecules. 2022;27:2186. doi: 10.3390/molecules27072186.

[71] Bocate KP, Reis GF, de Souza PC, Oliveira Junior AG, Durán N, Nakazato G, et al. Antifungal activity of silver nanoparticles and simvastatin against toxigenic species of *Aspergillus*. Intl J Food Microbiol. 2019;291:79–86. doi: 10.1016/j.ijfoodmicro.2018.11.012.

[72] Sherbiny GM, Moghannem SA, Sharaf MH. Antimicrobial activities and cytotoxicity of *Sisymbrium irio* L extract against multi-drug resistant bacteria (MDRB) and *Candida albicans*. Int J Curr Microbiol App Sci. 2017;6:1–13.

[73] Feskanich D, Ziegler RG, Michaud DS, Giovannucci EL, Speizer FE, Willett WC, et al. Prospective study of fruit and vegetable consumption and risk of lung cancer among men and women. J Natl Cancer Inst. 2000;92:1812–23. [PubMed: 11078758].

[74] Walters DG, Young PJ, Agus C, Knize MG, Boobis AR, Gooderham NJ, et al. Cruciferous vegetable consumption alters the metabolism of the dietary carcinogen 2-amino-1-methyl-6-phenylimidazo [4,5-b] pyridine (PhIP) in humans. Carcinogenesis. 2004;25:1659–69. [PubMed: 15073045]. Women. J Natl Cancer Inst. 2000;92:1812–23.

[75] Liu RH. Potential synergy of phytochemicals in cancer prevention: mechanism of action. J Nutr. 2004;134:3479S–85S.

[76] Drewnowski A, Gomez-Carneros C. Bitter taste, phytonutrients, and the consumer: a review. Am J Clin Nutr. 2000;72:1424–35.

[77] Holst B, Williamson G. A critical review of the bioavailability of glucosinolates and related compounds. Nat Prod Rep. 2004;21:425–47.

[78] Zhang Y. Cancer-preventive isothiocyanates: measurement of human exposure and mechanism of action. Mutat Res. 2004;555:173–90.

[79] Higdon JV, Delage B, Williams DE, Dashwood RH. Cruciferous vegetables and human cancer risk: epidemiologic evidence and mechanistic basis. Pharmacol Res. 2007;55(3):224–36. doi: 10.1016/j.phrs.2007.01.009.

[80] Singh RP, Ramarao P. Cellular uptake, intracellular trafficking and cytotoxicity of silver nanoparticles. Toxicol Lett. 2012;213:249–59.

[81] Li L, Tsao R, Yang R, Liu C, Zhu H, Young JC. Polyphenolic profiles and antioxidant activities of heartnut (*Juglans ailanthifolia Var. cordiformis*) and Persian walnut (*Juglans regia* L.). J Agric Food Chem. 2006;54:8033–40.

[82] Park EJ, Yi J, Kim Y, Choi K, Park K. Silver nanoparticles induce cytotoxicity by a Trojan-horse type mechanism. Toxicol In Vitro. 2010;24(3):872–8.

[83] Wypij M, Czarnecka J, Swiecimska M, Dahm H, Rai M, Golinska P. Synthesis, characterization and evaluation of antimicrobial and cytotoxic activities of biogenic silver nanoparticles synthesized from *Streptomyces xinghaiensis* OF1 strain. World J Microbiol Biotechnol. 2018;4:23.

[84] Sarkar S, Kotteeswaran V. Green synthesis of silver nanoparticles from aqueous leaf extract of Pomegranate (*Punica granatum*) and their anticancer activity on human cervical cancer cells. Adv Nat Sci Nanosci Nanotechnol. 2018;9:1.

[85] Juarez-Moreno K, Gonzalez EB, Girón-Vazquez N, Chávez-Santoscoy RA, Mota-Morales JD, Perez-Mozqueda LL, et al. Comparison of cytotoxicity and genotoxicity effects of silver nanoparticles on human cervix and breast cancer cell lines. Hum Exp Toxicol. 2017;36:931–48.